Supplementary information for "Laser-induced ultrafast demagnetization in the presence of a nanoscale magnetic domain network"

Boris Vodungbo,[1] Julien Gautier,[1] Guillaume Lambert,[1] Anna Barszczak Sardinha,[1,2] Magali Lozano,[1] Stéphane Sebban,[1] Mathieu Ducousso,[3] Willem Boutu,[3] Kaigong Li,[4] Bharati Tudu,[4] Marina Tortarolo,[4] Ranjit Hawaldar,[4] Renaud Delaunay,[4] Victor López-Flores,[5] Jacek Arabski,[5] Christine Boeglin,[5] Hamed Merdji,[3] Philippe Zeitoun,[1] and Jan Lüning[4]

[1)] *Laboratoire d'Optique Appliquée, ENSTA ParisTech – CNRS UMR 7639 – École polytechnique, Chemin de la Hunière, 91761 Palaiseau, France*

[2)] *Grupo de Lasers e Plasmas - Instituto de Plasmas e Fusão Nuclear, Instituto Superior Técnico, Av. Rovisco Pais, 1049-001 Lisbon, Portugal*

[3)] *CEA-Saclay, IRAMIS, Service des Photons, Atomes et Molécules, 91191 Gif-sur-Yvette, France*

[4)] *Laboratoire de Chimie Physique – Matière et Rayonnement, Université Pierre et Marie Curie – CNRS UMR 7614, 11 rue Pierre et Marie Curie, 75005 Paris, France*

[5)] *Institut de Physique et de Chimie des Matériaux de Strasbourg, CNRS UMR 7504 – Université de Strasbourg, 23 rue du Loess, 67034 Strasbourg, France*

(Dated: 13 July 2012)

CONTENTS

SUPPLEMENTARY FIGURES

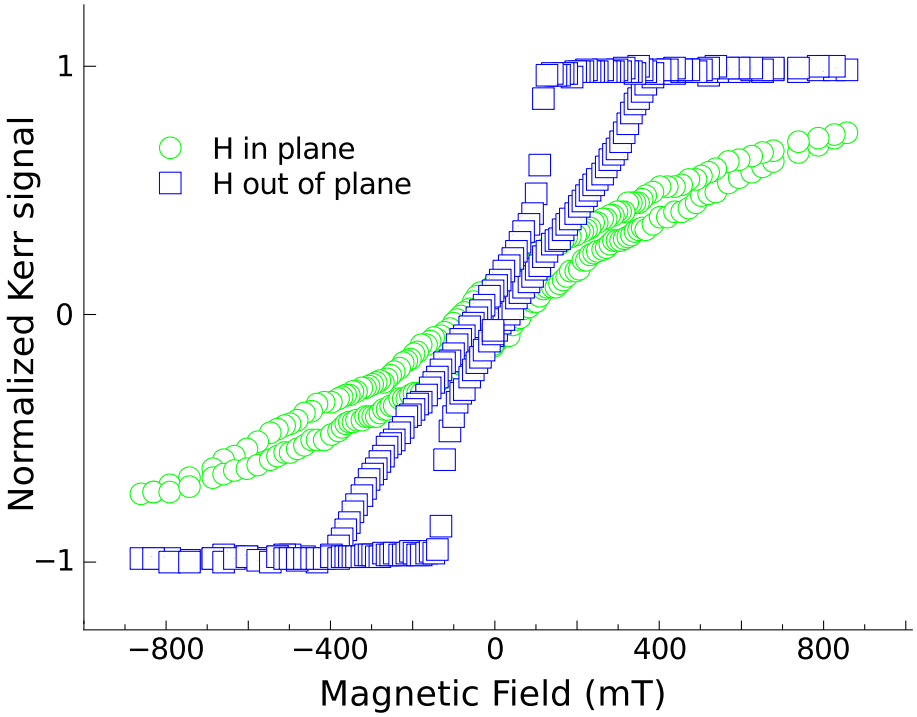

Supplementary Figure S1 | $[Co/Pd]_{30}$ multilayer film magnetic properties. Magnetization hysteresis loops, in and out of plane, recorded respectively in longitudinal and polar MOKE geometry. The out of plane magnetic anisotropy can be readily observed.

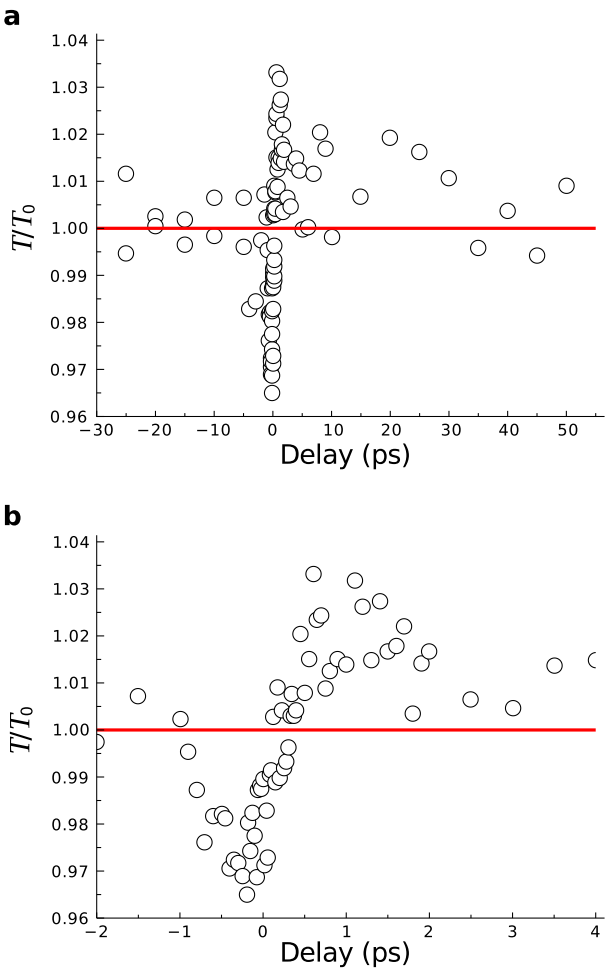

Supplementary Figure S2 | Evolution of the sample transmission after excitation by a femtosecond infrared pluse. (**a**) The sample transmission normalized to the unpumped mean transmission (T_0) has been plotted as a function of time delay (for a pump fluence of $7.5\ \mathrm{mJ/cm^2}$). Small fluctuations are observed with a maximum deviation of $\pm 4\ \%$ from T_0 and a standard deviation of $1.6\ \%$. These fluctuations are similar to the variations of the unpumped transmission itself ($\pm 3\ \%$ peak-to-peak and $1.4\ \%$ rms, not shown here), which are due to drifts in the HHG yield. This indicates that within the resolution of our experiment we do not observe any significant modification of the sample transmission. (**b**) Zoom into the zero delay region showing that the dip observed begins 1 ps before time zero. In view of our time resolution of about 40 fs, this reinforces the fact that the fluctuation of the transmission around zero delay (as the bump around 20 ps) have no physical meaning other than the variation of the probe beam. The red lines in panel a and b are guides to the eye.

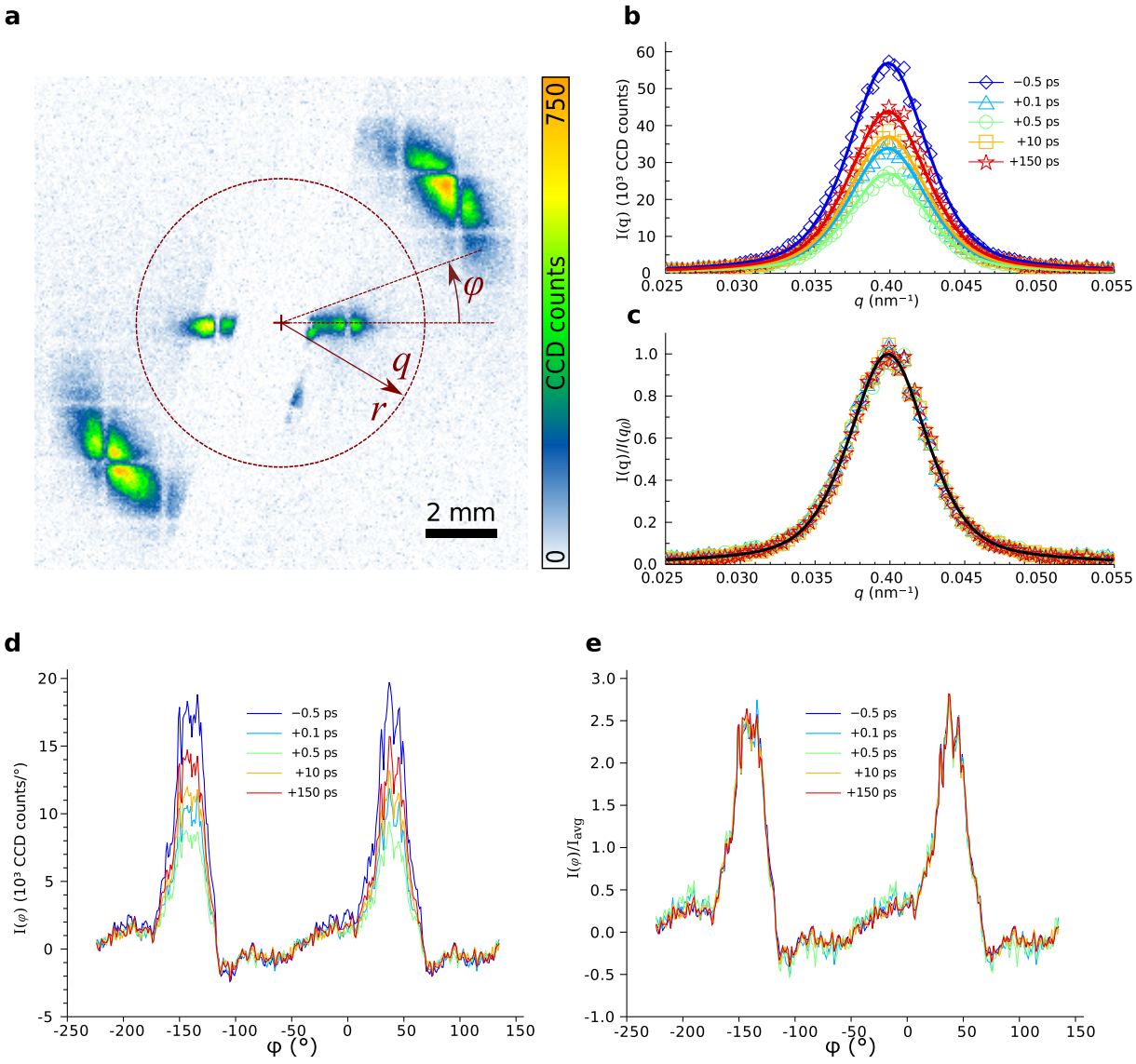

Supplementary Figure S3 | Scattered intensity as a function of wave vector transfer or of azimuthal angle. (**a**) Resonant magnetic scattering pattern of the unpumped sample showing r, q and ϕ. (**b,c**) Radial integration, $I(q)$, showing the scattered intensity (and the normalized intensity) as a function of q for different time delay. (**d,e**) Azimuthal integration, $I(\phi)$, showing the scattered intensity (and the normalized intensity) as a function of ϕ for different time delay. The total scattering intensity is given either by the integral of $I(q)$ or by the integral of $I(\phi)$.

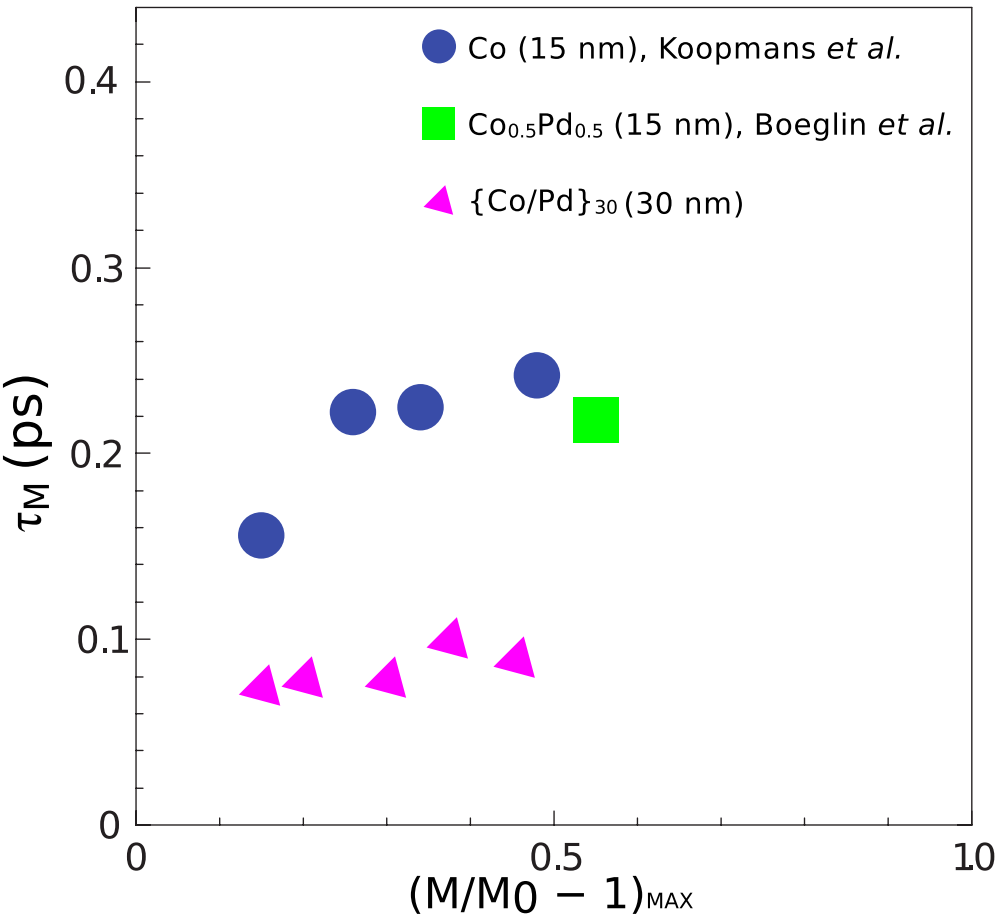

Supplementary Figure S4 | Thermalization time as a function of maximum demagnetization. Thermalization times reported for a 15 nm thin Co film (ref. 11) and for a 15 nm thin $Co_{0.5}Pd_{0.5}$ film (ref. 20) compared to the thermalization times of our $[Co(0.4\ nm)/Pd(0.6\ nm)]_{30}$ film. The latter are clearly shorter than the former.

SUPPLEMENTARY TABLES

fluence (mJ)	4	6	7.5	9	11
$(M/M_0-1)_{\min}$ (%)	-14	-21	-29	-37	-44
$\tau_{\rm th}$ (fs)	110 ± 25	95 ± 15	90 ± 15	110 ± 10	100 ± 15
$\tau_{\rm M}$ (fs)	75 ± 20	80 ± 15	80 ± 15	100 ± 10	95 ± 25
$\tau_{\rm s-ph}$ (ps)	1.1 ± 0.2	2.2 ± 0.3	3.3 ± 0.6	4.4 ± 0.9	5.6 ± 1
K_1	0.19 ± 0.02	0.24 ± 0.01	0.32 ± 0.01	0.39 ± 0.01	0.46 ± 0.04
K_2	0.05 ± 0.005	0.08 ± 0.005	0.14 ± 0.01	0.23 ± 0.01	0.29 ± 0.01

Supplementary Table S1 | Best fit parameters and associated standard deviation obtained for the [Co(0.4 nm)/Pd(0.6 nm)]$_{30}$ multilayer film. $\tau_{\rm th}$, $\tau_{\rm s-ph}$, K_1, K_2 and their associated error bars are directly obtained by the fitting procedure. $\tau_{\rm M}$ and $(M/M_0-1)_{\min}$ are calculated using the best fit parameters. The error bar on $\tau_{\rm M}$ is calculated by varying all the fit parameters within their standard variation.

fluence (mJ)	6	9
$(M/M_0-1)_{\mathrm{min}}$ (%)	-15	-31
τ_{th} (fs)	125 ± 25	120 ± 15
τ_{M} (fs)	85 ± 15	100 ± 20
$\tau_{\mathrm{s-ph}}$ (ps)	0.9 ± 0.2	2.5 ± 1.2
K_1	0.21 ± 0.02	0.35 ± 0.02
K_2	0.07 ± 0.005	0.15 ± 0.01

Supplementary Table S2 | Best fit parameters and associated standard deviation for the 50 nm thin CoPd alloy film. τ_{th}, $\tau_{\mathrm{s-ph}}$, K_1, K_2 and their associated error bars are directly obtained by the fitting procedure. τ_{M} and $(M/M_0-1)_{\mathrm{min}}$ are calculated using the best fit parameters. The error bar on τ_{M} is calculated by varying all the fit parameters within their standard variation.